Synthesis and Characterization of a Polymer/Multiwalled Carbon Nanotube Composite and Its Application in the Hydration of Ethylene Oxide

Fengping Yu, Hong Cai, Wenjun He, Weimin Yang, Zaiku Xie

Shanghai Research Institute of Petrochemical Technology, Shanghai 201208, China

Received 9 April 2009; accepted 3 September 2009
DOI 10.1002/app.31382
Published online 26 October 2009 in Wiley InterScience (www.interscience.wiley.com).

ABSTRACT: Multiwalled carbon nanotubes (MWNTs) were incorporated into the crosslinking network of a styrene–divinylbenzene copolymer (PS–DVB) via suspension polymerization. The prepared crosslinking PS–DVB with MWNTs was first treated with chloromethyl methyl ether to introduce chloromethyl groups through Friedel–Craft reaction; then, the chloromethylation product was reacted with trimethyl amine to obtain the target polymer/carbon nanotube composite: PS–DVB/MWNT ion-exchange resin. The obtained composite was characterized by Fourier transform infrared spectroscopy, thermogravimetric analysis, Raman spectroscopy, and X-ray photoelectron spectroscopy. The results show the successful incorporation of MWNTs into the polymer network. The physical and chemical properties of the PS–DVB/MWNT ion-exchange resin were nearly the same as those of the controlled sample. With its excellent antiswelling properties, the catalytic behavior of the polymer composite was examined in the hydration of ethylene oxide. Also, it demonstrated excellent stability as a catalyst without a decline in conversion and selectivity in a long-time run. © 2009 Wiley Periodicals, Inc. J Appl Polym Sci 115: 2946–2954, 2010

Key words: catalysts; composites; radical polymerization

INTRODUCTION

Carbon nanotubes (CNTs), a promising material, have been in the focus of various fields, such as physics, materials science, and engineering.[1–4] Because of their high length-to-diameter ratio and the π–π connection among adjacent carbons, CNTs have high flexibility, chemical stability, and electrical conductivity. Also, they have shown possible applications in the fields of energy storage, molecular electronics, nanomechanical devices, and composite materials. Also, they have prompted intensive scientific research. Particularly, polymer/CNT composites have been the focus of research since the first coverage of CNTs.[5,6] Experimentally incorporating CNTs into a polymer matrix can increase the mechanical properties at low concentration and electrical conductivity of the matrix.[7–11] By this incorporation method, the merits of the CNTs and the polymer can be integrated or enhanced, and the unique properties of the CNT can also be fulfilled efficiently, which makes it a useful approach.

Because of the increasing demand for monoethylene glycol (MEG), the hydration of ethylene oxide (EO) has attracted great scientific and industrial interest for a long time. Noncatalytic and catalytic hydrations of EO are two well-known approaches for the preparation of MEG. Numerous catalysts, including anion-exchange resins, quaternary phosphonium halides, polymeric organosilane ammonium salts, and macrocyclic chelating compounds, have been prepared for the catalytic hydration of EO to MEG. Also, a large fraction of studies covered the use of catalysts immobilized on an ion-exchange resin (IER).[12–14] However, the catalyst stability is a major challenge because the resins swell under reaction conditions.[15,16] No industrialization of catalytic hydration has been achieved because of the problems of catalysis. Therefore, the development catalysts with high thermal stability and high selectivity and conversion is urgent.

According to the articles published so far on the heterogeneous catalytic hydration of EO, polymeric IERs, both strong acid and strong basic types, are the most effective catalysts. The acidic hydration process is accompanied by serial reaction. On the other hand, alkali hydration, with fewer byproducts, can increase the MEG selectivity; thus, it has obtained more research interest. However, the intrinsic problem of the swelling of IERs as the hydration proceeds restricts their application in the industrialization of the catalytic hydration of EO. Measures such as increasing the crosslinking density have been used to solve the swelling

Correspondence to: F. Yu (yufp@sript.com.cn).

problem to some extent at the cost of reducing the exchange capacity and the number of active sites of the resin.

Here we report a brand new way to handle the problem of swelling, as mentioned previously. A styrene–divinylbenzene copolymer (PS–DVB)/multiwalled carbon nanotube (MWNT) IER composite was prepared via the *in situ* suspension polymerization of styrene (St), divinylbenzene (DVB), and CNT, followed by chloromethylation and amination, as described in the Experimental section. Also, the obtained polymer/CNT composites were carefully characterized by means of thermal analysis, Fourier transform infrared (FTIR) spectroscopy, X-ray photoelectron spectroscopy (XPS), and the measurement of the antiswelling and catalytic properties. The final resin incorporated with CNTs had improved antiswelling capability, whereas the total amount of active reaction sites remained constant, and the stability and the conductivity of the catalyst increased as well.

EXPERIMENTAL

Materials

Styrene (China National Pharmaceutical, Shanghai, China, 99%) and DVB (China National Pharmaceutical, 99%) were washed by an NaOH solution (5% w/w) and saturated sodium chloride solution three times to remove inhibitors, then washed with deionized water, stirred over magnesium sulfate overnight and then over calcium hydride, distilled, and stored under a nitrogen atmosphere at 4°C. The purification of dibenzoyl peroxide (BPO; China National Pharmaceutical, 98%) was carried out by recrystallization from methanol solution. Gelatin, poly(vinyl alcohol) (PVA), Tween 80, zinc chloride, chloromethyl methyl ether, trimethyl amine solution (≥33%), and 1,2-dichloroethane (≥99%) were purchased from Sinopharm Chemical Reagent Co., Ltd., and were used as received. MWNTs were purchased from Nafine Chemical Industry Group Co., Ltd., baked to remove amorphous carbon at 300°C for 1 h in an air atmosphere, and dispersed in water to remove water-soluble impurities before use in the polymerization.

Synthesis of the PS–DVB/MWNT IER composites

The polymer/MWNT composites were synthesized via a modified suspension polymerization. In a typical polymerization, St (57.5 g), DVB (5.0 g), Tween 80 (0.5 g), and the initiator BPO (0.3 g) were placed in a 250-mL, round-bottom flask, and then, the flask was placed in an oil bath at 60°C for 1.5 h. The pristine MWNTs (2.5 g) were then added to the flask, and this process continued for another 1 h. The obtained monomer mixture was then added to the water phase, which consisted of gelatin (1.3 g), PVA (1.0 g), and deionized water (130 mL), after it was dissolved at 40°C. The stirring rate was modified to control the diameter of the polymer composite. Slowly, the temperature was raised to 78–80°C, and the polymerization proceeded for 5–6 h. Then, the mixture was kept at 85–86 and 95–96°C for 5 h, respectively. The obtained polymer composite was washed by hot water and dried at 90°C until a constant weight was reached.

Chloromethylation and amination of the PS–DVB/MWNT IER composites

The Friedel–Craft reaction was used to introduce chloromethyl groups to the crosslinking network of the polymer/MWNT composites. The composite (18.0 g) and chloromethyl methyl ether (75 mL) were mixed together to swell the crosslinked polymer for 4 h at room temperature. Then, $ZnCl_2$ (7.2 g) was added to the mixture in two batches. The reaction was allowed to proceed at 38–40°C for 10 h. The chloromethylation product was washed by acetone and dried until a constant weight was reached.

The chloromethylation product (12.0 g) was first immersed in 48 mL of 1,2-dichloromethyl methyl ether to swell for 2 h at room temperature. Trimethyl amine solution (12 mL, ≥33%) was added, and the reaction ran for 4 h at 30°C. After the reaction, the mixture was diluted with deionized water until the density reached 1 g/mL. Then, it was washed with dilute hydrochloride solution, deionized water, and dilute NaOH solution in sequence. The final product was dried at 90°C until a constant weight was reached for further use.

Synthesis and modification of the PS–DVB crosslinking polymer

The PS–DVB crosslinking polymer was synthesized via a conventional suspension polymerization. The feed ratio of St to DVB was same as that of the polymer/MWNT composite; thus, the crosslinking density was the same as well. St (57.5 g), DVB (5.0 g), and BPO (0.3 g) were placed in a flask first and stirred for a while until they dissolved. Then, the gelatin solution (1% w/w) was added, and the polymerization first ran for 4 h at 80°C and then at 85 and 95°C for 2 h, respectively. Also, the chloromethylation and amination of the obtained product were carried out with the same conditions as used for the polymer/MWNT composite.

Measurement of the swelling extent

The polymer/MWNT composite was first immersed in ethanol for 4 h and washed. Then, it was

immersed in a 2*M* solution of dilute HCl and dilute NaOH and washed with deionized water until the pH reached 7. This pretreated polymer/MWNT composite (10 mL) was first centrifuged at 2500 rpm and then loaded into a 100-mL pressure bomb. The volume of the sample was recorded as V_1. After 20 mL of ethylene glycol solution (25%, v/v) and 5 mL of EO were added, the pressure bomb was sealed and put into an oven at a constant temperature of 85°C for 100 h. The mixture inside was centrifuged at 2500 rpm, and the volume was measured and recorded as V_2.

Measurement of the total exchange capacity

The total exchange capacity was measured according to National Standard of People's Republic of China GB/T 5760-2000, which describes the determination of the exchange capacity of anion-exchange resins in hydroxylic form. The methodology was as follows: the sample was first pretreated according to National Standard of People's Republic of China GB/T 5476. Then, it was washed with a dilute hydrochloride solution, deionized water, and a dilute NaOH solution in sequence to obtain PS–DVB/MWNT IER in hydroxylic form; this was further used in the catalytic hydration of EO. W_1 (usually 2.0–2.5 g) of the prepared sample was measured and soaked in a 100-mL solution of hydrochloric acid [c_1 (*M*)] at 40°C for 2 h. A 25-mL soak solution was taken and titrated with V_1 (mL) of sodium hydroxide solution [c_2 (*M*)]. The total exchange capacity was calculated according to eq. (1):

$$\text{Total exchange capacity} = \frac{100c_1 - 4c_2V_1}{W_1(1 - X)} \quad (1)$$

where c_1 is the density of the hydrochloric acid solution (mol/L), c_2 is the density of the sodium hydroxide solution (mol/L), V_1 is the volume of the sodium hydroxide solution used in the titration, W_1 is the weight of PS–DVB/MWNT IER measured, and X is the water content of PS–DVB/MWNT IER measured according to the National Standard of People's Republic of China GB/T 5759-2000.

Characterization

FTIR spectra were recorded on a Nicolet 5700 spectrometer (Thermo Nicolet, Madison, WI). The samples were ground thoroughly with potassium bromide (KBr) at approximately 1–2 wt %, and the resulting powder was pressed into a transparent pellet. A total of 20 scans taken at a 4-cm^{-1} resolution were averaged.

Thermogravimetric analysis (TGA) was conducted on a TA 4000 TGA 2050 (Waters Technologies (Shanghai) Limited, Shanghai, China) from room temperature to 900°C at a heating rate of 20°C/min under a nitrogen atmosphere. The differential scanning calorimetry (DSC) analyses were performed with a TA 4000 DSC 2190 with nitrogen as the purge gas from room temperature to 200°C at a rate of 10°C/min.

The XPS experiments were carried out on a RBD upgraded PHI-5000C ESCA system (PerkinElmer, USA) with Mg Kα radiation ($E h\nu = 1253.6$ eV). The sample was directly pressed to a self-supported disk (10×10 mm^2), mounted onto a sample holder, and then transferred into the analyzer chamber. The binding energies were calibrated with the containment carbon ($C_{1s} = 284.6$ eV). Raman spectra were obtained on a LABRAM-HR with an argon-ion laser at an excitation wavelength of 514.5 nm (Horiba Jobin Yvon Inc., USA).

RESULTS AND DISCUSSION

The PS–DVB/MWNT IER composite and controlled samples (PS–DVB IER) with a crosslinking density of 8% were prepared under the same conditions by suspension polymerization and after chloromethylation and amination. The crosslinking density (CD) was controlled via the monomer feed ratio according to the following equation.

$$\text{CD} = \frac{m_{\text{DVB}} + m_{\text{St}}}{m_{\text{St}}} \times 100\% \quad (2)$$

where m_{DVB} and m_{St} represent the weight of DVB and St added to the reaction mixture.

To examine the successful preparation of the strongly basic PS–DVB/MWNT IER, the samples were first characterized by FTIR spectroscopy, as shown in Figure 1. For comparison, the figure also includes the spectra of the MWNTs and the controlled sample in hydroxylic form [Fig. 1(e)]. The appearance of a weak and broad band at about 3400 cm^{-1} in the spectrum of the MWNTs [Fig. 1(a)] was attributed to the presence of —OH groups on the surface of the as-received MWNTs and was believed to result from ambient atmospheric moisture tightly bonded to the MWNTs.[17,18] The spectrum of the PS–DVB/MWNT polymer composite [Fig. 1(b)] exhibited characteristic vibration bands for PS–DVB in KBr. The peaks at 3025, 1602, 1492, 1450, 756, and 698 cm^{-1} were attributed to the phenyl group. The peaks at 2922 and 2850 cm^{-1} were attributed to the methylene and methenyl groups, and the peaks at 1028 cm^{-1} were attributed to the C—Ph groups. This suggests the presence of the PS–DVB crosslinked polymer in the functionalized MWNTs.

Figure 1(c,d) shows the FTIR spectra of the chloromethylated PS–DVB/MWNT polymer composite

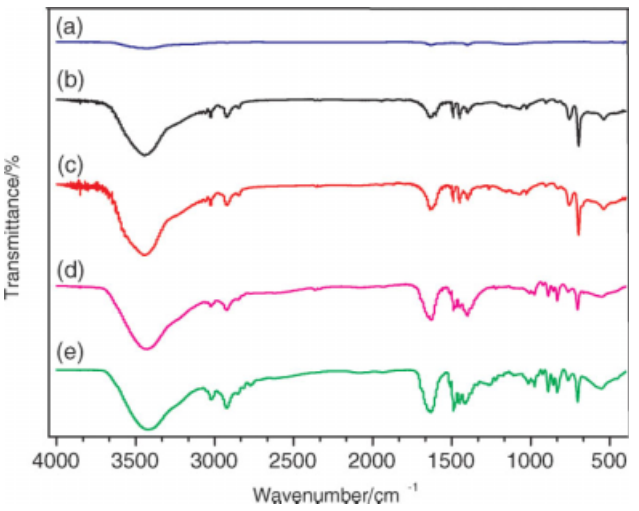

Figure 1 FTIR spectra of the (a) pristine MWNTs, (b) PS–DVB/MWNT polymer composite, (c) chloromethylated PS–DVB/MWNT polymer composite, (d) PS–DVB/MWNT IER composite in its hydroxylic form, and (e) controlled sample in its hydroxylic form. [Color figure can be viewed in the online issue, which is available at www.interscience.wiley.com.]

and the PS–DVB/MWNT IER composites in hydroxylic form, respectively. In addition to the characteristic vibration bands for PS–DVB in KBr, new peaks appeared in Figure 1(c). The absorption peak located at 1263 cm^{-1} was related to the in-plane bending vibration of C—Ph groups after chloromethylation. The peaks at 676 cm^{-1} were attributed to the C—Cl groups, and the peaks at 1413 cm^{-1} were related to the bending vibration of C—H in the —CH_2Cl group incorporated into the polymer network after chloromethylation. However, the peaks at 676 cm^{-1} disappeared in the spectrum of the PS–DVB/MWNT IER composites in hydroxylic form [Fig. 1(d)]. New peaks appeared at 970 cm^{-1} because of the replacement of the C—Cl group by C—N groups after successful amination. In addition, the peaks at 1395 cm^{-1} became stronger because more —CH_3 groups were incorporated into the polymer composites. The FTIR results suggest the successful functionalization of the MWNTs with polymer chains.

The prepared PS–DVB/MWNT IER composites were typical strongly basic IERs, and the characteristic data are shown in Table I. The data show that PS–DVB IER and the PS–DVB/MWNT IER composites had nearly the same properties, including particle density, water content, mean particle size, and total exchange capacity, which demonstrated that the fundamental structures of the PS–DVB/MWNT IER composites were nearly identical.

TGA was carried out to better understand the decomposition process and the thermal stability of the prepared polymer/CNT composites. The weight loss curves of three samples, the pristine MWNTs, the PS–DVB IER, and the PS–DVB/MWNT IER are delineated in Figure 2. The pristine MWNTs showed an onset decomposition temperature around 500°C in air, and the complete decomposition was achieved at approximately 720°C, whereas they started to decompose around 800°C under a nitrogen atmosphere, as shown in Figure 2 (gray line and purple line). The TGA results reveal that PS–DVB IER and the composite showed similar decomposition behavior under a nitrogen atmosphere. There were two peaks indicating that the decompositions were followed by two steps, the evaporation of water and the decomposition of PS–DVB network. A weight loss of about 9% was observed for both PS–DVB IER and the composite because of the evaporation of the free water in IER from room temperature to about 80°C. This evaporation process continued to 250 and 340°C for PS–DVB IER and the composite separately until the water was fully evaporated. The difference between PS–DVB IER and the composite was thought to be derived from the MWNTs incorporated into the crosslinking network. However, there was actually no difference in the water content in the network of the PS–DVB polymer. The decomposition of the crosslinking network was same as PS–DVB. The final sample leftover for the composite was about 4%, which was in accordance with the feed ratio in the preparation of the polymer composite.

The PS–DVB IER and the PS–DVB/MWNT IER composite were also characterized by DSC (figures not shown). T_g increased from 125 to 132°C, 7° higher, when the MWNTs were incorporated into the crosslinking network of PS–DVB, which was more evidence for the successful functionalization of the MWNTs.

Raman spectroscopy is one of the most extensively used means for characterizing the extent of disorder or the degree of crystallinity in the functionalized

TABLE I
Total Physical and Chemical Properties of the PS–DVB IER and PS–DVB/MWNT IER Composites in the Hydroxylic Form

Sample	Particle density (g/mol)	Water content (%)	Mean particle size (mm)	Total exchange capacity (mmol/g)
Pure PS–DVB IER	1.08	40–50	0.42	3.4
PS–DVB/MWNT composite (8%)	1.09	40–50	0.40	3.3

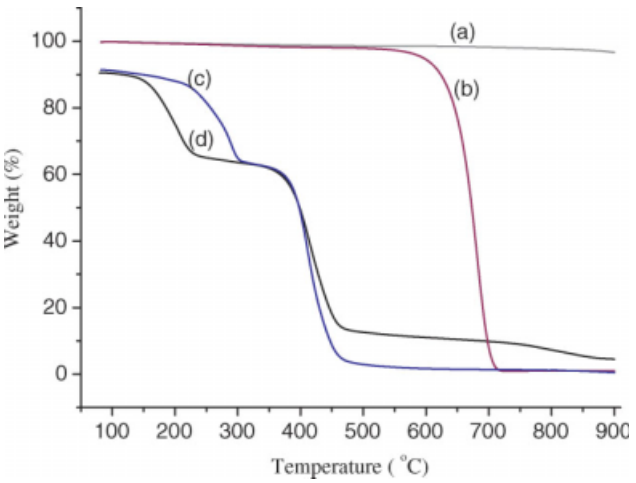

Figure 2 TGA curves of the (a) pristine MWNTs in nitrogen, (b) pristine MWNTs in air, (c) PS–DVB IER, and (d) PS–DVB/MWNT IER composite with a crosslinking density of 8%. [Color figure can be viewed in the online issue, which is available at www.interscience.wiley.com.]

MWNTs.[19–21] Usually, direct evidence of the covalent bonding of CNTs can be demonstrated through Raman spectroscopy. The two kinds of bands CNTs possess are the disorder band (D-band) peak at approximately 1350 cm^{-1} and the graphitic band (G-band) at approximately 1580 cm^{-1}. The D-band and G-band represent the C—C single bond and C=C double bond, respectively. The Raman results are plotted in Figure 3. The area ratio of the D-band and G-band for the MWNTs and the PS–DVB/MWNT IER composite with a crosslinking density of 8% were 1.30 and 1.55, respectively. The existence of the D-band and G-band indicated that during the polymerization, the graphite structure of the MWNTs was not destroyed and that the number of sp^3 hybridized carbon atoms increased.[22–24] As shown in the spectrum, the D-band was enhanced, and the polymer chain radicals or the initiator fragment was attached to the sidewall of the MWNTs. This indicated partial destruction of the conjugation structures of the sidewall of the MWNTs due to the addition of a small molecular free radical or the polymer chain free radical during the suspension polymerization. This result is similar to other research findings on covalent bonding of CNTs. The absorption spectrum of the PS–DVB/MWNT IER composite red-shifted compared with that of the pristine MWNTs. The peaks shifted from about 1331 and 1586 cm^{-1} to about 1322 and 1574 cm^{-1} for the D-band and G-band, respectively.[25–27] This was attributed to the decrease in the electronic interaction between MWNTs. When incorporated into the polymer network of PS–DVB, the π electron system of the pristine MWNTs was disturbed; on the other hand, the polymer chains wrapped on the surface of the MWNTs also prohibited the transition of electrons between MWNTs.[28–30]

In addition, XPS analysis was used to determine the surface composition of the MWNTs. The typical information depth of XPS is about 5 nm. Survey XPS spectra of the pristine MWNTs and PS–DVB/MWNT IER composite are shown in Figure 4, respectively. Samples were degassed overnight within the XPS chamber (5×10^{-8} Pa) before analysis.

As shown in Figure 4, both spectra revealed the presence of carbon and oxygen. The presence of oxygen in the pristine MWNTs was ascribed to the atmospheric oxidation of residual oxides resulting from the purification process and was consistent with the FTIR results discussed previously. There were two brand new peaks, chloride (199.8 eV) and

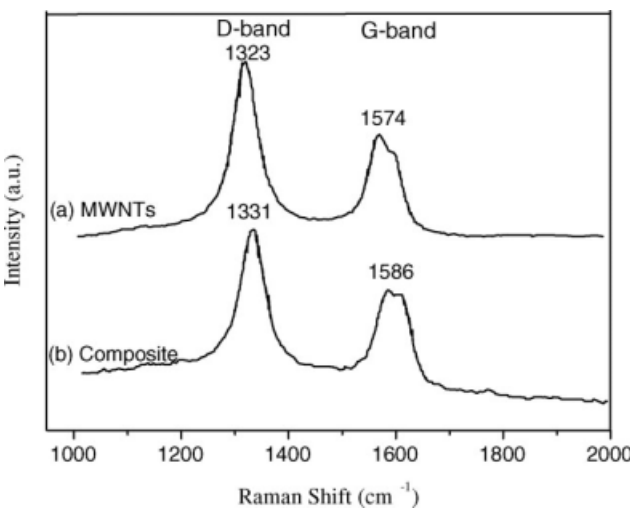

Figure 3 Raman spectra of the (a) pristine MWNTs and (b) PS–DVB/MWNT IER composite.

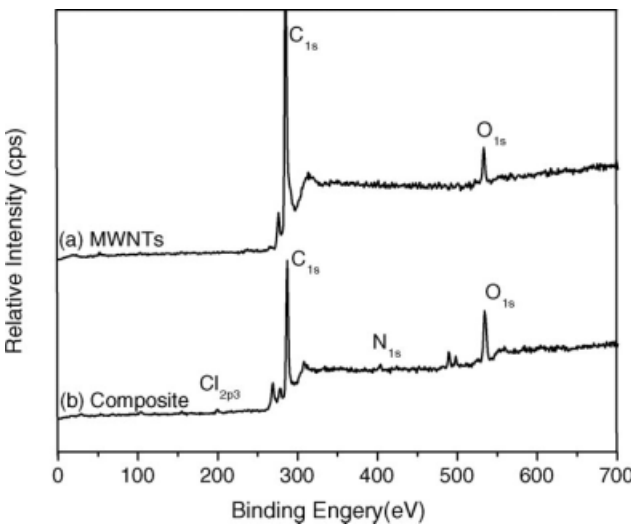

Figure 4 XPS full-scan spectra of the (a) pristine MWNTs and (b) PS–DVB/MWNT IER composite in its hydroxylic form.

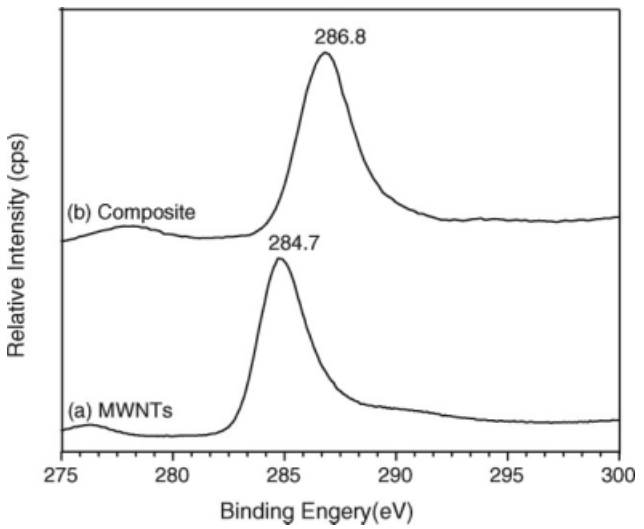

Figure 5 Narrow C_{1s} XPS spectra of the (a) pristine MWNTs and (b) PS–DVB/MWNT IER composite in its hydroxylic form.

nitrogen (403.6 eV), that appeared in the spectra of the PS–DVB/MWNT IER composite. The presence of N_{1s} was attributed to the $N^+(CH_3)_3OH^-$ group attached to the polymer chain. Another peak appearing at 200 eV was Cl_{2p3}, which resulted from the residual chloride atoms in the amination product. However, the relative atomic concentration of chloride was minimal and would not affect its catalysis in the hydration of EO. This also suggested the successful amination and synthesis of the polymer/MWNT composite.

The narrow-scan spectra of the C region are shown in Figure 5. The main C—C peak appeared at 284.7 eV for the pristine MWNTs in Figure 5(a). Also, an additional photoemission present at higher binding energy for the pristine MWNTs indicated the presence of functional groups bonded to the surface. The main peak for the PS–DVB/MWNT IER composite appeared at 286.8 eV, which was 2.1 eV higher than that of the pristine MWNTs [see Fig. 5(b)]. This was interpreted by the transition of C=C bond with high binding energy to the C—C bond with low binding energy, which was more proof of the incorporation of MWNTs into the PS–DVB cross-linking network.

IERs are largely used in the electricity, chemical, and food industries. The status of the application of IERs as catalysts or catalyst precursors in organic syntheses was reviewed by Georges Gelbard.[31] As a strongly basic IER, the catalytic properties of the polymer/MWNT composite in the hydration of EO were studied extensively.

Industrially, the molar ratio of water to EO has to be in the range 22–25 to acquire high conversion and selectivity. Accompanying this is the problem of postfractionation of a large amount of water in the crude product, which requires quantitative water vapor and a large volume of separation equipment. Figure 6 plots the effect of the molar ratio of water to EO on the hydration of EO. As shown in Figure 6, the selectivity increased from 95.6 to 97.0% as the molar ratio increased from 8 to 22. On the other hand, the conversion invariably stayed above 99.2%, even close to 100%, when the molar ratio was 8.

The effect of temperature on the hydration of EO is further drawn in Figure 7. It shows a converse trend in conversion and selectivity when compared with the effect of the molar ratio of water to EO. The main reason was that at low temperature, the obtained MEG was not quantitatively enough to achieve the by-reaction; thus, the selectivity was high. As the temperature increased, more MEG was

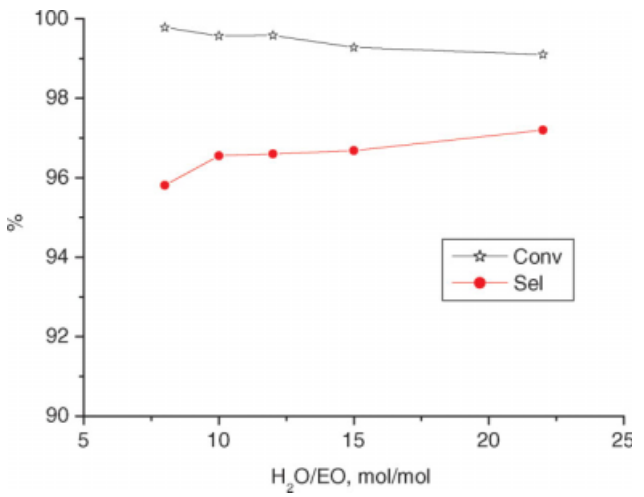

Figure 6 Effect of the molar ratio of water to EO on the catalytic hydration of EO. [Color figure can be viewed in the online issue, which is available at www.interscience.wiley.com.]

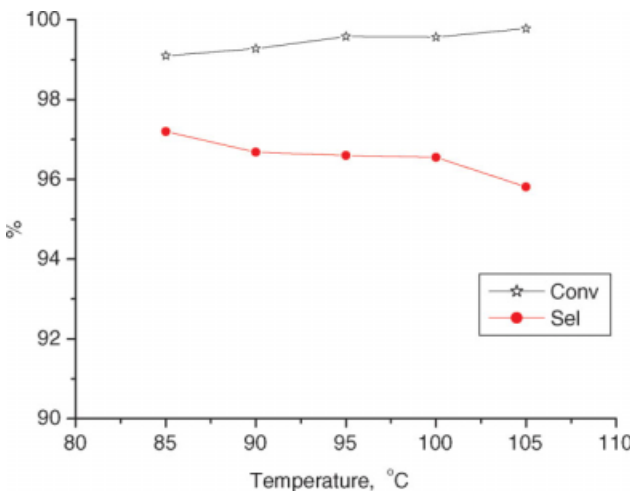

Figure 7 Effect of temperature on the catalytic hydration of EO. [Color figure can be viewed in the online issue, which is available at www.interscience.wiley.com.]

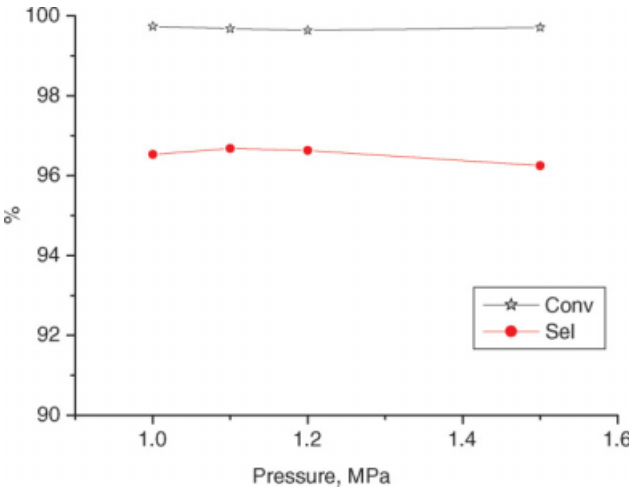

Figure 8 Effect of pressure on the catalytic hydration of EO. Conv and Sel represent the conversion and selectivity of EO in the catalytic hydration of EO. [Color figure can be viewed in the online issue, which is available at www.interscience.wiley.com.]

produced, and the concentration of MEG in the reactor increased, which means that the conversion increased. Meanwhile, it also facilitated side reactions, which reduced the selectivity of MEG. However, the selectivity of hydration was still as high as 96% at 105°C.

The pressure had the least influence on the hydration of EO, as shown in Figure 8. In the range 1.0–1.5 MPa, the conversion and the selectivity changed little, with values remaining as high as 99.5 and 96%, respectively.

The antiswelling properties of the prepared PS–DVB/MWNT IER composite was analyzed by experiment, as described in the Experimental section. As mentioned in the Introduction, the antiswelling properties are crucial to the long-time catalytic hydration of EO. The extents of swelling for the controlled sample and the polymer/MWNT composite were calculated according to eq. (3):

$$A = \frac{V_2 - V_1}{V_1} \times 100\% \quad (3)$$

where A is the swelling extent and V_1 and V_2 represent the volumes of the sample before and after swelling in the mixture of ethylene glycol (20 mL, 25%) and EO (5 mL) at 85°C for 100 h. The obtained swelling extents were 5.9 and 2.7% for PS–DVB IER and the polymer/MWNT composite, respectively; this demonstrated that the latter had superior antiswelling properties. Therefore, it is better for the long-time catalytic application in the hydration of EO, on the condition that the basic characteristics of the IER, such as the total exchange capacity, water content, and crosslinking density, are nearly the same.

As we know, the antiswelling capabilities are of great importance to IERs when they are used as catalysts in the hydration of EO. The volume of the catalyst expands several times because of the swelling of the IER in the catalytic hydration; this, thus, decreases the catalyst's strength greatly.[32] What is worse, the catalyst would break into fragments and block the reactor.

The catalytic behavior of the controlled sample as a catalyst for EO hydration is shown in Figure 9. The catalyst was prepared according to National Standard of People's Republic of China GB/T 5760-2000. The test lasted 200 h because of the pressure increase inside the reactor from 1.2 MPa at the beginning to 10 MPa after 200 h. We assumed that the pressure increase was due to the swelling of the controlled sample under the reaction conditions. As shown in Figure 9, the conversion invariably remained at a high level, nearly 99.7% during the whole test. However, the selectivity was just 87.5% at the beginning and gradually decreased to about 73.91% at the end of the test. This was ascribed to the relatively low heat resistance of the controlled sample. As the test went on, the lost of active sites increased under the reaction temperature (90°C), and the controlled sample lost its catalytic strength, which resulted in the decrease in selectivity.

The long-time run of the polymer composite as a catalyst in the hydration of EO was carried out for 2200 h on stream, and the recorded data are plotted in Figure 10 for comparison. During the catalytic test, the polymer composite demonstrated excellent stability without an obvious decline in conversion and selectivity, which invariably remained at values of 99.5 and 97.2%, respectively, as shown in Figure 10. Thus, the incorporation of MWNTs in the crosslinking network increased the stability of the

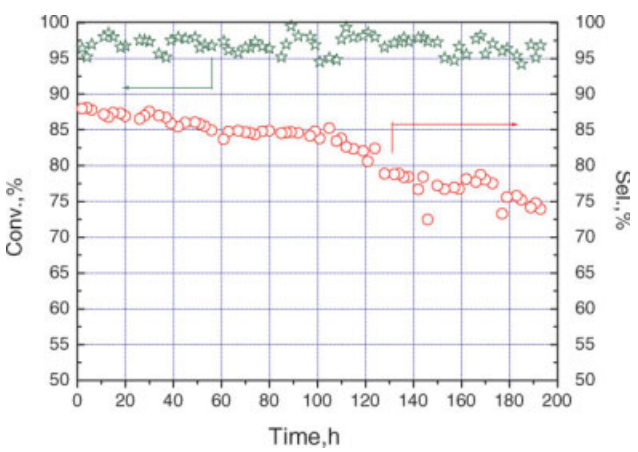

Figure 9 Catalytic behavior of the controlled sample as a catalyst in EO hydration. [Color figure can be viewed in the online issue, which is available at www.interscience.wiley.com.]

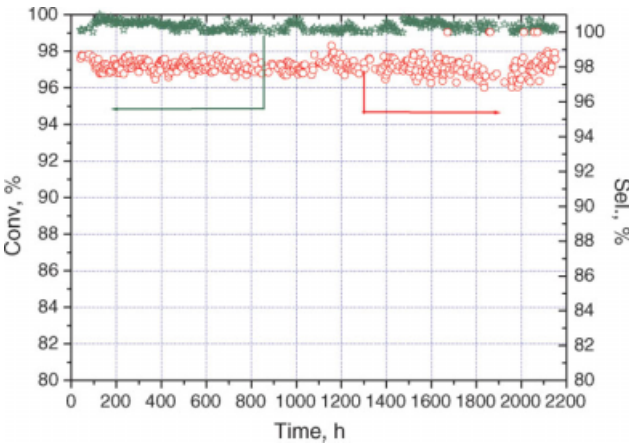

Figure 10 Conversion and selectivity of EO catalyzed by PS–DVB/MWNT IER within 2200 h. [Color figure can be viewed in the online issue, which is available at www.interscience.wiley.com.]

polymer and the capability to keep the active site loss at a low level; this is of great significance in the hydration of EO.

Thus, we successfully established that MWNTs could be conveniently incorporated into the crosslinking network of PS–DVB IER via conventional radical polymerization. This technique is expected to be suitable for the industrial scale-up preparation of polymer/CNT composites. The content of MWNTs can reach 4% and the crosslinking density can be 8%, equal to that of industrialized nonfunctionalized IERs.

Among researches, two main methodologies, the grafting-onto and grafting-from techniques, have been developed for the purpose of increasing the solubility of CNTs in organic or aqueous solvents.[22,33–35] For the grafting-onto methodology, reports have pointed out the interaction of CNTs with radicals or polymer anions. This includes the preparation of a polymer chain with a specific molecular weight and the following reaction of the polymer chain end (polymeric radicals or polymer anions) with the graphite surface of CNTs. In this process, the CNTs are first modified by oxidation, esterification, and so on to incorporate specific reactive end groups that will react with the polymer chain end. However, this was not the case in our study, which could be seen clearly. The MWNTs were used as received, and the tedious modification steps were excluded.

The grafting-from methodology is based on the immobilization of the polymer precursors on the surface of the CNTs and subsequent propagation of the polymerization in the presence of monomers.[36–38] It was first fabricated by the *in situ* polymerization process. Various research groups have reached the same results: that the initiator fragment is first attached to the double bond and the polymer chain is propagated from the surface of CNTs. The polymer chains incorporated on the surface of CNTs, either by grafting-from or grafting-onto methodology, help to dissolve the tubes in a wide range of solvents.[39]

In our case, the growing polymer chains, initiated by the thermal decomposition of dibenzoyl peroxide and subsequent polymerization, had a tendency to react with the unsaturated double bonds on the surface of MWNTs; also, it had the tendency to add the double bond of DVB. We could readily functionalize the MWNTs through the grafting-onto mechanism. The polymer chains were attached to the surfaces of MWNTs via covalent bonding. With the amount of double bonds taken into consideration, the MWNTs, together with DVB, might have played the role of a potential crosslinking agent. Thus, the real density of crosslinking was a little higher than the calculated one based on eq. (1). It is known that the higher the crosslinking density is, the more compact the structure and higher antiswelling capability the MWNTs possesses. The total exchange capacity decreased when the DVB/St feed ratio increased; however, it was not affected in the case of the polymer/MWNT composite preparation, which means that the MWNTs incorporated into the crosslinking network did not affect the chloromethylation and amination processes. However, the importance of MWNTs in the composite was not just limited to this on the basis of our research. It enhanced the thermal stability of the polymer, as demonstrated in the catalysis experiment.

CONCLUSIONS

Polymer/MWNT composites were successfully synthesized via the *in situ* suspension polymerization of St and DVB initiated by BPO. After chloromethylation and amination, the obtained product was carefully characterized by FTIR spectroscopy, Raman spectroscopy, XPS, and thermal analysis. The data suggested that the prepared composites had a similar structure as the controlled sample. Also, the pristine MWNTs, which acted as potential crosslinking agents, were dispersed well in the crosslinking network of the PS–DVB polymer. The obtained polymer/MWNT composites performed well in the catalysis experiment of the hydration of EO. The swelling extent of the catalyst decreased, and its thermal stability in the long-term run was greatly improved.

References

1. Iijima, S. Nature 1991, 354, 56.
2. Iijima, S.; Ichihashi, T. Nature 1993, 363, 603.

3. Wang, C. C.; Guo, Z. X.; Fu, S. K.; Wu, W.; Zhu, D. B. Prog Polym Sci 2004, 29, 1079.
4. Wang, C. Y.; Chen, T. G.; Chang, S. C.; Cheng, S. Y.; Chin, T. S. Adv Funct Mater 2007, 17, 1979.
5. Ajayan, P. M.; Stephan, O.; Colliex, C.; Trauth, D. Science 1994, 265, 1212.
6. Calvert, P. Nature 1999, 399, 210.
7. Schadler, L. S.; Giannaris, S. C.; Ajayan, P. M. Appl Phys Lett 1998, 73, 3842.
8. Qian, D.; Dickey, E. C.; Andrews, R.; Rantell, T. Appl Phys Lett 2000, 76, 2868.
9. Baughman, R. H.; Zakhidov, A. A.; de Heer, W. A. Science 2002, 297, 787.
10. Dai, L. M.; Mau, A. W. H. Adv Mater 2001, 13, 899.
11. Ha, J. U.; Kim, M.; Lee, J.; Choe, S.; Cheong, I. W.; Shim, S. E. J Polym Sci Part A: Polym Chem 2006, 44, 6394.
12. Sidney A.; Bernhard, E. G.; Louis P. H. J Am Chem Soc 1954, 76, 991.
13. Strickler, G. R.; Lee, G.-S. J.; Rierert, W. J. (The DOW Chemical Co.). U.S. Pat. 9,825,985 (1999).
14. Shvets, V. F.; Kozlovskiy, R. A.; Kozlovskiy, I. A.; Makarov, M. G.; Suchkov, J. P.; Koustov, A. V. Chem Eng J 2005, 107, 199.
15. Li, Y. C.; Yan, S. R.; Qian, L. P.; Yang, W. M.; Xie, Z. K.; Chen, Q. L.; Yue, B.; He, H. Y. J Catal 2006, 241, 173.
16. Van Hal, J. W.; Ledford, J. S.; Zhang, X. K. Catal Today 2007, 123, 310.
17. Ramanathan, T.; Fisher, F. T.; Ruoff, R. S.; Brinson, L. C. Chem Mater 2005, 17, 1290.
18. Xia, H. S.; Wang, Q.; Qiu, G. H. Chem Mater 2003, 15, 3879.
19. Rao, A. M.; Jorio, A.; Pimenta, M. A.; Dantas, M. S. S.; Saito, R.; Dresselhaus, G.; Dresselhaus, M. S. Phys Rev Lett 2000, 84, 1820.
20. Lin, Y.; Zhou, B.; Fernando, K. A. S.; Liu, P.; Allard, L. F.; Sun, Y. P. Macromolecules 2003, 36, 7199.
21. Fischer, D.; Potschke, P.; Brunig, H.; Janke, A. Macromol Symp 2005, 230, 167.
22. Umek, P.; Seo, J. W.; Hernadi, K.; Mrzel, A.; Pechy, P.; Mihailovic, D. D.; Forro, L. Chem Mater 2003, 15, 4751.
23. Qin, S. H.; Qin, D. Q.; Ford, W. T.; Resasco, D. E.; Herrera, J. E. Macromolecules 2004, 37, 752.
24. Zhao, X. D.; Fan, X. H.; Chen, X. F.; Chai, C. P.; Zhou, Q. F. J Polym Sci Part A: Polym Chem 2006, 44, 4656.
25. Dehonor, M.; Varlot-Masenelli, K.; Gonzalez-Montiel, A.; Gauthier, C.; Cavaille, J. Y.; Terrones, H.; Terrones, M. Chem Commun 2005, 5349.
26. Skakalova, V.; Dettlaff-Weglikowska, U.; Roth, S. Diamond Relat Mater 2004, 13, 296.
27. Peng, J.; Qu, X. X.; Wei, G. S.; Li, J. Q.; Qiao, J. L. Carbon 2004, 42, 2741.
28. O'Connell, M. J.; Bachilo, S. M.; Huffman, C. B.; Moore, V. C.; Strano, M. S.; Haroz, E. H.; Rialon, K. L.; Boul, P. J.; Noon, W. H.; Kittrell, C.; Ma, J. P.; Hauge, R. H.; Weisman, R. B.; Smalley, R. E. Science 2002, 297, 593.
29. Heller, D. A.; Barone, P. W.; Swanson, J. P.; Mayrhofer, R. M.; Strano, M. S. J Phys Chem B 2004, 108, 6905.
30. Dresselhaus, M. S.; Dresselhaus, G.; Jorio, A.; Souza, A. G.; Saito, R. Carbon 2002, 40, 2043.
31. Gelbard, G. Ind Eng Chem Res 2005, 44, 8468.
32. Wang, F.; Chen, J. L.; Chen, Q.; He, M. Y.; Zhang, Y. F. J Mol Catal (China) 2006, 20, 97.
33. Banerjee, S.; Hemraj-Benny, T.; Wong, S. S. Adv Mater 2005, 17, 17.
34. Ying, Y. M.; Saini, R. K.; Liang, F.; Sadana, A. K.; Billups, W. E. Org Lett 2003, 5, 1471.
35. Tasis, D.; Tagmatarchis, N.; Bianco, A.; Prato, M. Chem Rev 2006, 106, 1105.
36. Hong, C. Y.; You, Y. Z.; Pan, C. Y. J Polym Sci Part A: Polym Chem 2006, 44, 2419.
37. Yoon, K. R.; Kim, W. J.; Choi, I. S. Macromol Chem Phys 2004, 205, 1218.
38. Liu, Y. Q.; Yao, Z. L.; Adronov, A. Macromolecules 2005, 38, 1172.
39. Jia, Z. J.; Wang, Z. Y.; Xu, C. L.; Liang, J.; Wei, B. Q.; Wu, D. H.; Zhu, S. W. Mater Sci Eng A 1999, 271, 395.